EFFECT OF TRACE ADDITION ON THE MICROSTRUCTURAL DEGRADATION OF Cu-Zn-Al SHAPE MEMORY ALLOY

A. K. Bhuniya, S. Datta, P. P. Chattopadhyay and M. K. Banerjee

Department of Metallurgy, B. E. College (Deemed University), Howrah 711 103, India.

ABSTRACT

The effect of trace addition of Zr, Ti and misch metal (MM) on the grain growth kinetics of Cu-Zn-Al shape memory alloy with reference to pinning caused by the precipitates at low temperature ageing and solute drag mechanisms. It been demonstrated that solute drag mechanism favoured nucleation of variants and grain refinement.

INTRODUCTION

Grain refinement of the shape memory alloys (SMA) is an effective measure for remarkable improvement of mechanical properties as the grain boundaries provide the potential sites for release of strain [1]. In this regard, addition of some selected elements in minor amount has been found useful for controlling the grain size due to favored formation of precipitate phase as well as retardation of the grain growth kinetics. Among the various technological properties influenced by grain growth, degradation of shape memory effect in several alloys has been identified as the issue of major concern [2]. Several attempts have been made to achieve fine grain structure, particularly in Cu-based SMAs by trace addition of Ti, Zr, B, V, etc. [1-3]. Earlier, Wang et al. have studied the effect of Ti, Zr, B and Fe on the grain growth kinetics of CuZnAl shape memory alloy by utilizing modulated differential scanning calorimetry [4]. The contribution of the trace elements has been attributed to the formation of the precipitate phase, interactions with quenched in vacancies and tendency towards segregation at the grain boundaries [5]. On the other hand the favorable effect provided by the precipitate phases may well be objected due to their influence on the value of percent recoverable strain during subsequent transformation cycle [6,7].

In this regard, pinning of grain boundaries by precipitate phases and solute drag effect caused by the impurity atom may be responsible primarily for controlling the boundary migration process [8,9]. The aim of this work is to study age hardening and grain growth behavior of Zr, MM and Ti added Cu-Zn-Al SMAs at appropriate temperatures by measuring the variation of microhardness as a function of ageing temperature for a given duration. Formation of the precipitate phase at different levels of temperature has been observed initially by carrying out optical micrography of the aged alloys. Subsequently, some of the significant results of the optical micrography have been substantiated by TEM. On the other hand grain growth kinetics has been studied within a temperature range from 800°C to 950°C to see the effect of solute drag mechanism in the absence of particle pinning.

EXPERIMENTAL

The alloys (Table 1) were induction melted, cast, hot rolled to 2 mm sheets and then cut into samples approximately 10 x 3 x 70 mm. The rolled samples were isothermally annealed at the β-phase region (825°C) for 30 min. duration followed by ice water quenching. Phase transformation was studied by differential scanning calorimetry (using a STA 625 instrument at a heating rate of 10°C/min) with the as quenched samples. The representative transformation temperatures obtained from the thermograms are presented in table 2. One set of the annealed samples was subjected to isochronal ageing treatment at 75°C, 250°C and 300°C while the other set was subjected to annealing at 800°C, 850°C and 900°C for the study of grain growth. Age hardening behavior of different alloys was studied by measuring the micro hardness using Microduramet attached with a Polyver Met metallograph. Optical metallography was carried out using a Versamet 2 microscope after etching the samples with acidified $FeCl_3$ solution. The precipitate behavior was studied in details by transmission electron micrography under a Philips microscope. Grain size of the annealed samples was measured by intercept method incorporating appropriate correction factor.

Table 1 : Chemical composition (Wt %) of the SMAs

Alloy	Cu	Zn	Al	Ti	Zr	MM
A	77.31	13.70	8.99	-	-	-
B	77.10	13.90	8.95	-	-	0.05
C	78.00	12.80	8.90	-	0.30	-
D	78.30	12.80	8.80	0.10	-	-

Table 2 : Transformation temperatures (°C) of different SMAs

Alloy	As	Af	Tp
A	65	122	77
B	22	74	44
C	15	66	42
D	10	41	23

RESULT AND DISCUSSION

Fig. 1 shows the micro hardness obtained for 2h-aged. It is apparent that higher peak-hardness was achieved in the case of alloys C and B. It is interesting to note that the peak hardness values are achieved within a close temperature range for all the alloys. This is indicative of the fact that precipitation process in alloys B-D follows the similar trend as that of alloy A. In contrast, average aging effect in the case of alloy D (Ti added) is greater than those for the alloys C and B (Zr and MM added). It is also apparent from Fig. 1 that in the case of alloy A micro hardness

value decreases after 75°C due to the rearrangement of dislocation in the martensite phase as predicted earlier for similar alloy [10]. Subsequently, the micro hardness value increases after 150°C and attains a maximum value at 250 °C followed by softening upto the level of the initial value (that obtained at 75 °C). The observed softening beyond 250°C is due to dissolution of precipitate during the later stage of ageing process conducted at higher level of temperature say, 300°C.

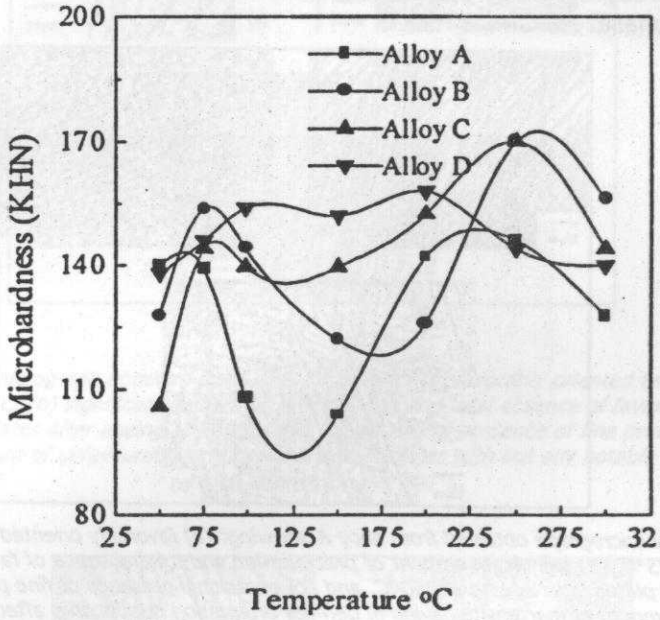

Fig. 1 : Age hardening curves for alloys A, B, C and D. Two stage hardening in the case of the trace added alloys may be noted.

Interestingly, Fig. 1 reveals two-stages of hardening which are distinctly separated in the case of trace added alloy. The first stage hardening may be attributed to the ageing effect in the parent phase due to the probable order recovery process occurring in the parent phase observed in the case of similar alloys at lower level of ageing temperature [11]. While at higher levels of temperature such recovery process gradually ceases, the process of nucleation and growth of the precipitates gradually becomes dominant and the samples attain the peak-aged condition.

Figs. 2-5 reveal the optical micrograph of alloys A-D obtained after ageing of the samples at different levels of temperatures. It is revealed that ageing at 75°C does not bring in any significant precipitation in any of the alloys. It is also evident that in all the alloys habit plane variants and lattice invariant twins are restored during the martensitic transformation. It may also be noted that orientation relationship that occur through type-1 twins, yielding the spear-head morphology of martensite [12], is better restored in the case of alloys B-D (Fig. 3-5) than in alloy A (Fig. 2). It may also be recorded from Figs. 2-5 that maximum precipitate density

is achieved after ageing at 250°C (i.e., at the peak aged condition) for all the concerned alloys. It may be predicted that such an extensive precipitation may change the composition of the parent phase in a manner such that the matrix at room temperature may even contain a significant amount of non-martensitic phaseś. The micrographs obtained from the alloys at 300°C demonstrates much reduced density of precipitates due to dissolution of the same within the allowed ageing duration thereby resulting into a microstructure with appreciable population of martensitic phase.

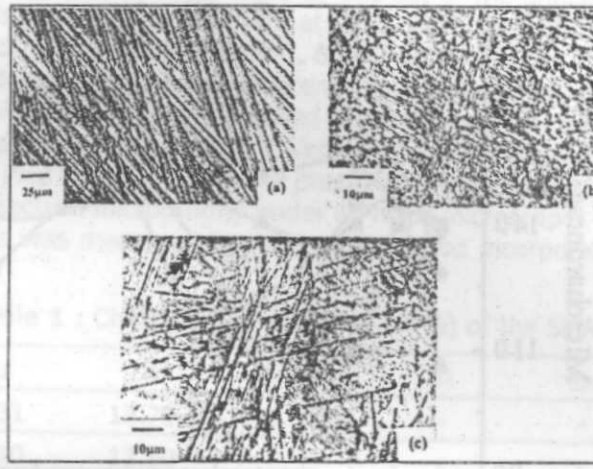

Fig. 2 : Optical micrograph obtained from alloy A showing: (a) favorably oriented twin variants after ageing at 75°C, (b) significant amount of precipitation and total absence of favorably oriented martensite plates after ageing at 250°C, and (c) occasional presence of fine precipitates with reasonable amount of martensite having ill defined orientation relationship after ageing at 300°C.

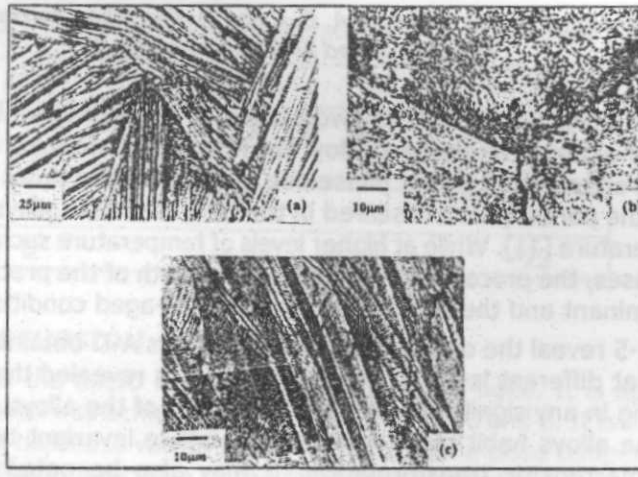

Fig. 3 : Optical micrograph obtained from alloy B showing: (a) favorably oriented twin variants after ageing at 75°C, (b) significant amount of precipitation and total absence of favorably oriented martensite plates after ageing at 250°C, and (c) occasional presence of fine precipitates with notable presence of favorable martensite variants and ill-defined LSA after ageing at 300°C.

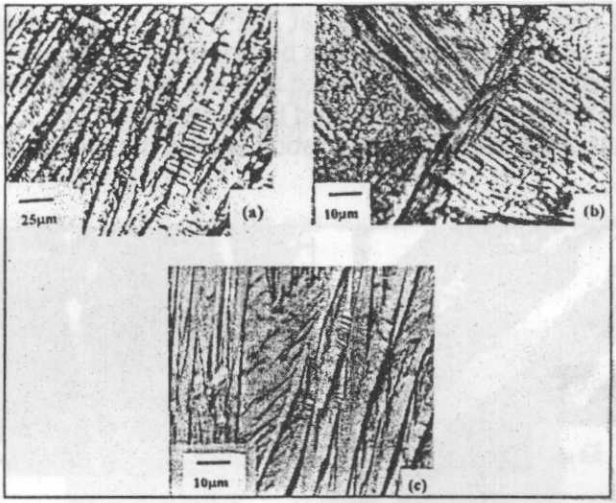

Fig. 4 : Optical micrograph obtained from alloy C showing: (a) favorably oriented twin variants after ageing at 75°C, (b) significant amount of precipitation and total absence of favorably oriented martensite plates after ageing at 250°C, and (c) occasional presence of fine precipitates with reasonable amount of unfavourably oriented martensite plates with out any notable presence of LAS twins after ageing at 300°C.

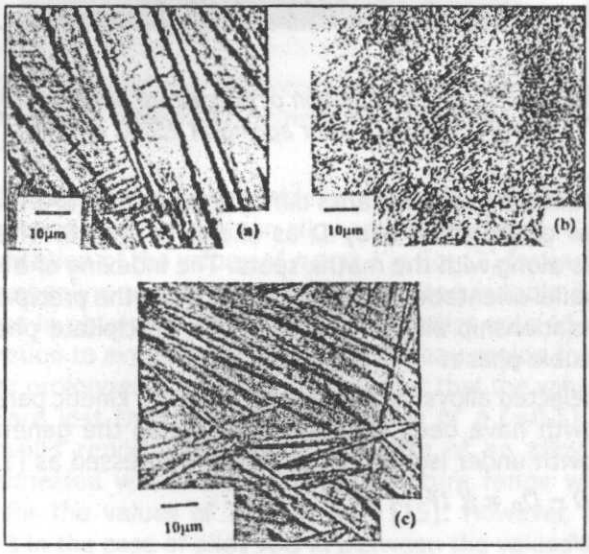

Fig. 5 : Optical micrograph obtained from alloy D showing: (a) favorably oriented twin variants after ageing at 75°C, (b) significant amount of precipitation and total absence of favorably oriented martensite plates after ageing at 250°C, and (c) occasional presence of fine precipitates with reasonable amount of spear headed martensite after ageing at 300°C.

Fig. 6 shows the transmission electron micrograph of alloy A (Fig. 6 (a)) alloy C (Fig. 6 (b)) and alloy D (Fig. 6 (c)) aged at 250°C for 2 h . It is clearly evident that significant amount of precipitate phase has been formed at the peak aged condition for all the concerned alloys. It may be noted that the precipitate particles formed in alloys C and D are relatively finer compared to those formed in alloy A. Moreover, a reasonable amount of dislocation concentration around the precipitate particles may be observed

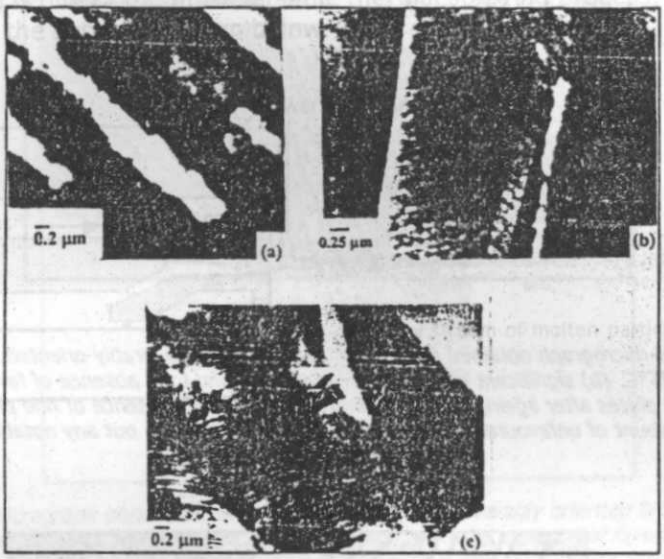

Fig. 6 : TEM micrograph showing formation of precipitate phase in (a) alloy A (b) alloy C and (c) alloy D after ageing at 250°C for 2 h.

Fig. 7 presents the selected area diffraction pattern (SADP) obtained from the precipitate phase observed in alloy D as shown in Fig. 6. The SADP shows the precipitates spots along with the matrix spots. The indexing of the pattern reveals a cube to cube parallel orientation relationship between the precipitate and the matrix phase. Such a relationship allows to identify the precipitate phase presumably as Cu_2AlT_i type of cubic phase.

In all the selected alloys in the present study the kinetic parameters concerned to the grain growth have been determined by using the generalized equation of normal grain growth under isothermal condition expressed as [13]:

$$D - D_0 = K t^n \quad (1)$$

or,

$$\ln (D - D_0) = \ln K + n \ln t \quad (2)$$

where, Do is the initial grain diameter, D is the average grain diameter measured after annealing at a given level of temperature for a given duration, t is the time,

and K and n are constants. The constant n is identified as growth order normally having a maximum value of 0.5 for ultra high pure metals at a temperature near the melting temperature [13]. However, departure from the maximum value occur due to interaction, solute drag effect etc. On the other hand, K exhibits a temperature dependence which may be expressed by relationship [14].

$$K = K_0 \exp^{(-Q/RT)} \quad (3)$$

Where, K_0 is frequency factor, R is the gas constant, Q is the activation energy, and T is absolute temperature.

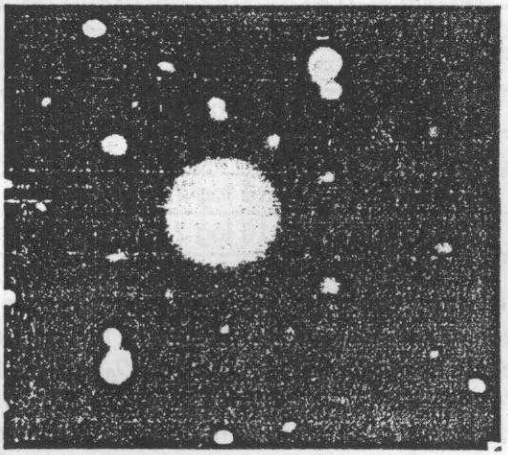

Fis 7 : Shows the SADP obtained from the precipitate phase shown in Fig. 7. Note a cube to cube parallel orientation relationship between the precipitate and the matrix phase

The values of n and K are determined from the slope and intercept respectively, of the *ln (D - Do)* versus t plots for a given alloy and temperature. Growth equations obtained after substitution of the values of *n* and *K* in Eq. (2) for each of the present alloys at different annealing temperatures are presented in table 3. It is important to mention here that in obtaining *n* and *K* growth kinetics upto 15 mins have been taken into consideration to avoid the effect of the plateau region that occur in the *D* versus *t* curves after prolonged annealing. It is evident that the values of *n* obtained for the base alloy are less than the maximum value of *n* (=0.5) [13]. This is in contrast to the results reported earlier in the case of an alloy of comparable composition and annealed within a similar temperature range which revealed a positive deviation for the values of *n* (n > 0.5) [15]. However, the values of *n* presented in Table 3 in the case of alloy A is in between the values of *n* reported for the commercial brass alloy (0.2 to 0.3) and high purity brass (0.4 to 0.6) [16]. It is also apparent from table 3 that addition of Zr, MM and Ti induces further lowering of the values of n in comparison to that of the base alloy. This may be attributed to the additional kinetic impediments introduced by the trace elements.

Table 3 : Parameters concerned with the determination of grain growth kinetics

Alloy	Temparature	Growth Equation (T°C)	Growth order	Activation energy (kJ/mol)
A	800	log D=1.9+0.37 log t	0.37	36.0
	850	log D=1.8+0.35 log t	0.35	
	900	log D=2.00+0.30 log t	0.30	
B	800	log D=1.98+0.21 log t	0.21	63.7
	850	log D =2.06+0.19 log t	0.19	
	900	log D=2.18+0.14 log t	0.14	
C	800	log D=1.88+0.26 log t	0.26	52.5
	850	log D=1.98+0.24 log t	0.24	
	900	log D=2.11+0.14 log t	0.14	
D	800	log D=2.20 +0.20 log t	0.20	80.7
	850	log D=2.18+0.18 log t	0.18	
	900	log D=2.22+0.10 log t	0.10	

The activation energy values (Q) for grain growth in case of each of the alloys have been determined by substituting the value of ln K, obtained from Eq. (3), into Eq. (2) and subsequently taking the slope of $ln(D - D_0)$ versus 1/T plots. The values of Q obtained for different alloys are tabulated in Table 3. It may be noted that the values of$(D - D_0)$ at different temperatures have been recorded at t = 10 min (i.e., close to point of inflection of the individual curve) with a view to rule out the effect of initial inhomogeneities in the matrix on the values of Q. It is apparent from Table 3 that addition of the trace elements has resulted into remarkable increase in the values of Q m comparison to that of the base alloy A. It is important to mention here that the value of Q obtained from alloy A is marginally less than that reported earlier for a similar alloy (43 kJ/mol) [17] determined within a temperature range 700 - 730°C. In contrast, Guilemany et al. [15] have reported a much higher value (120 - 160 kJ/mol) determined within a tmperature range 750 - 900°C. It is further apparent from Table 3 that the values of Q obtained for the trace added alloys increases in the order Ti, MM and Zr depending on their role in impediment of the grain boundary migration mainly through solute drag mechanism. It is also interesting to record that the highest activation energy value obtained in the case of Ti added alloy is in close agreement with that obtained earlier in the case of similar alloy after trace addition of Ti and B (80 kJ/mol) [17].

In the present study an attempt has also been made to understand the effect of trace element on the grain growth behavior in terms of variation of velocity (dD/dt) as a function of 't' as shown in Fig. 8. It is apparent that at any given value of time within the duration of grain growth, dD/dt increases in the reverse order to that of increase in Q. It may also be noted that the values of t at which dD/dt

approaches zero increases in the similar order to that of increase in dD/dt. It is important to mention here that determination of dD/dt is not restricted on the nature of variation of D as a function of t at any level of time within the given range of duration, whereas determination of Q essentially necessitates an Arrhenius behavior within the range of t selected for the determination of Q. Therefore, it is apparent that the dD/dt versus t plots may reasonably be utilized for the qualitative understanding of the grain growth kinetics.

Table 3 and Fig. 8 reveal that the trace elements exert significant effect in retarding grain growth process in the present alloys. In the absence of particle pinning effect the significant grain refinement effect may be attributed to the enhanced solute drag effect due to the presence of Ti, Zr and MM. It may be recorded here that all the chosen trace elements in the present study are potential oxide formes and their oxides are reasonably stable at the selected range of temperature (i.e., 800 - 900°C). Therefore probable pinning effect due to the presence of the oxide particle in the matrix can not be ruled out. However, their influence in determining the relative effectiveness of the trace element in grain refinement is insignificant.

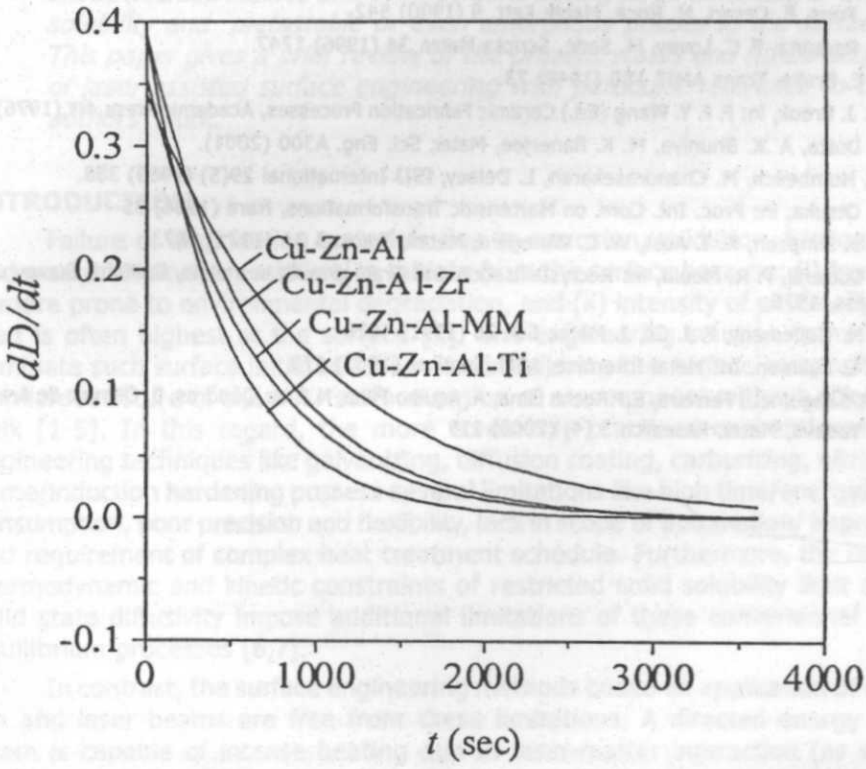

Fig. 8 : Variation of rate of change of average grain size (dD/dt) as a function of anealing time (t) for different alloys.

CONCLUSION

This investigation has demonstrated the effect of trace elements on the process of microstructural degradation an ageing. It has been shown that precipitation at the peak-aged condition induces the microstructural evolution in a manner, which is detrimental to the shape memory effect. However, trace addition resulted in some improvement in the nucleation of favoured variants even after ageing Zr appears to be most effective followed by MM and Ti.

It is also shown that the trace additions provide enhanced grain refinement effect primarily due to solute drag effect, Ti offers maximum benefit followed by MM and Zr.

REFERENCE

1. T. Tadaki, in: K. Otsuka, C. M. Wayman (Eds.), Shape Memory Materials, Cambridge Univ. Press, 1998, p. 112.
2. G. N. Sure, L. C. Brown, Metall. Trans. A 15A (1984) 1613.
3. G. N. Sure, L. C. Brown, Scripta Metall. 19 (1985) 401.
4. F. T. Wang, F. X. Chen, Z. G. Wei, D. Z. Yang, Scripta Metall. Matter. 25 (1991) 2565.
5. G. Gottstein, L. Shvindlerman, CRC Press, 1999, p. 133.
6. J. Pons, E. Cesari, M. Roca, Mater. Lett. 9 (1990) 542.
7. D. Roqueta, F. C. Lovey, M. Sade, Scripta Mater. 34 (1996) 1747.
8. J. E. Bruke, Trans AMIE 180 (1949) 73.
9. R. J. Brook, in: F. F. Y. Wang (Ed.) Ceramic Fabrication Processes, Academic Press, NY.(1976)p.331
10. S. Dutta, A .K. Bhuniya, M. K. Banerjee, Mater, Sci. Eng. A300 (2001).
11. V. Humbeeck, M. Chandrasekaran, L. Delaey, ISIJ International 29(5) (1989) 388.
12. K. Otsuka, in: Proc. Int. Conf. on Martensitic Transformations, Nara (1986) 35
13. C. J. Simpson, K. T. Aust, W. C. Winegard, Metall. Trans. A 2A (1971) 987.
14. P. Cotterill, P. R. Mould, in: Recrystallisation and Grain growth in metals, Guilford, Surrey univ. press, 1976.
15. J. M. Guilemany, F. J. Gil, J. Mater, Sci. 26 (1991) 4626
16. R. L. Fullman. In: Metal Interface, ASM. Seminar (1952) 179
17. RA-Sanguinetti Ferreira, E.P.Rocha Lima, A. Aquino Filho, N.F. de Quadros, 0. Olimpio de Araujo, Y. P. Yadava, Mater. Research 3 (4) (2000) 119